https://doi.org/10.5194/esd-2019-36
Preprint. Discussion started: 23 July 2019

Earth System Dynamics Discussions

Enhanced warming of seasonal cold extremes relative to the mean in the Northern Hemisphere extratropics

Mia H. Gross[a*], Markus G. Donat[a,b], Lisa V. Alexander[a], Steven C. Sherwood[a]

[a] Climate Change Research Centre and ARC Centre of Excellence for Climate Extremes, UNSW Sydney, Australia

[b] Barcelona Supercomputing Center, Barcelona, Spain

Correspondence to: Mia H. Gross (mia.gross89@gmail.com)

ORCID for M. H. Gross: 0000-0003-1589-6033

Abstract

Cold extremes are anticipated to warm at a faster rate than both hot extremes and average temperatures for much of the Northern Hemisphere. The consequences of warming cold extremes can affect numerous sectors, including human health, tourism and various ecosystems that are sensitive to cold temperatures. Using a selection of Global Climate Models, this paper explores the enhanced warming of seasonal cold extremes relative to seasonal mean temperatures in the Northern Hemisphere extratropics. The potentially driving physical mechanisms are investigated by assessing conditions on the day, or prior to, when the cold extreme occurs to understand how the different environmental fields are related. During winter months, North America, Europe and much of Eurasia show enhanced warming of cold extremes projected for the late 21st century, compared to the mid-20th century. This is shown to be largely driven by reductions in cold air temperature advection, suggested as a likely consequence of Arctic amplification. In spring and autumn, cold extremes are expected to warm faster than average temperatures for most of the Northern Hemisphere mid- to high-latitudes, particularly Alaska, northern Canada and northern Eurasia. In the shoulder seasons, projected decreases in snow cover and associated reductions in surface albedo are suggested as the largest contributor affecting the accelerated rates of warming in cold extremes. This study uses a novel approach to examine the day in which the extreme occurs to improve our understanding of the environmental conditions that contribute to the accelerated warming of cold extremes relative to mean temperatures.

Keywords: daily temperature, CMIP5, HadGHCND, snow cover, surface albedo, temperature advection

1. Introduction

Daily temperature extremes are expected to continue to warm, along with increases in the mean, as a consequence of increasing greenhouse gases in the atmosphere. The rates of warming of extremes and mean temperatures are, however, not uniform, and differ depending on the season and region. Disproportionate rates of warming for different parts of the temperature distribution imply a change in the shape of the distribution. This is significant because it effects the probability and frequency of extreme events (Mearns et al., 1984), which can cause widespread impacts on both human and natural ecosystems, more so than changes in the mean temperature alone (Intergovernmental Panel on Climate Change (IPCC), 2012).

https://doi.org/10.5194/esd-2019-36
Preprint. Discussion started: 23 July 2019

Earth System Dynamics Discussions
Open Access
EGU

Both observational data and climate model simulations suggest that cold extremes are warming faster than warm extremes for much of the globe (e.g. Kharin and Zwiers, 2005; Donat and Alexander, 2012; Donat et al., 2013). Studies have also shown that in recent decades, cold extremes have been warming at a faster rate than local mean temperatures for some regions in the Northern Hemisphere (Brown et al., 2008; Gross et al., 2018). The enhanced warming of cold extremes in these regions, relative to both the mean temperature and warm extremes, is indicative of decreasing variability in these regions during boreal winter (Screen, 2014; Ylhäisi and Räisänen, 2014; Schneider et al., 2015; Rhines et al., 2017). Climate model projections suggest this decrease in variability due to the accelerated warming of the coldest days will continue (Holmes et al., 2016), with some regions in the mid- to high-latitudes projected to increase over 5°C more than mean temperatures by the late 21st century (Gross et al., 2019). These disproportionate rates of warming suggest that changes in cold extremes are driven by mechanisms other than increases in local mean temperatures alone. A better understanding of the physical drivers related to the projected rates of enhanced warming of cold extremes is therefore crucial for assessing the probability and potential impacts of future changes in cold extremes.

The physical mechanisms driving the accelerated warming rates of cold extremes differ depending on the region and season. For land regions in the Northern Hemisphere mid- to high-latitudes, the warming of cold extremes and the associated decreases in temperature variability during winter months are consistent with reductions in cold air temperature advection that are a consequence of Arctic amplification (Screen, 2014; Schneider et al., 2015; Holmes et al., 2016; Rhines et al., 2017). Arctic amplification, a phenomenon describing the enhanced warming of the Arctic relative to lower latitudes (Serreze and Francis, 2006), has been suggested as one of the dominant causes of the observed and projected reductions in the severity of extremely cold days during winter in the Northern Hemisphere extratropics (Screen, 2014; Schneider et al., 2015; Holmes et al., 2016; Rhines et al., 2017). This effect on cold extremes from Arctic amplification is shown to be a consequence of northerly winds from the Arctic bringing warmer than usual air to more southerly regions on the coldest days, which are warming faster than the warm days, therefore reducing the sub-seasonal temperature variability (Screen, 2014; Holmes et al., 2016). Though it seems relatively clear that changes in temperature advection are linked with decreases in temperature variability in many mid- to high-latitude Northern Hemisphere regions, there is still uncertainty as to its role in driving the enhanced warming of seasonal cold extremes relative to the corresponding seasonal mean. It is more likely that multiple factors are influencing the differences in seasonal and regional warming rates.

Aside from changes in atmospheric circulation patterns and thermal advection that may be altering cold extremes, variations in surface fluxes affecting the overall surface energy budget have strong links with surface temperatures and extremes. In particular, changes in snow cover play an important role in altering surface temperature in Northern Hemisphere regions that experience snowfall (e.g. Cohen and Rind, 1991; Mote, 2008; Diro et al., 2018). The high reflectivity and thermal emissivity of snow, compared to other natural surfaces, increases the surface albedo, lowers the absorbed shortwave radiation at the surface, and increases shortwave radiation reflected at the surface (Cohen and Rind, 1991). The surface albedo feedback from snow cover is more likely to influence winter months and early spring in the Northern Hemisphere, where snow accumulation is at its highest (He et al., 2014; Thackeray et al., 2015; Diro et al., 2018). However, the effect of snow cover on surface temperature is suggested to be strongest during spring when snow melt is at its highest, leading to increases in latent heat at the surface (Cohen and Rind, 1991; Dutra et al., 2011; Xu and Dirmeyer, 2011; Diro et al., 2018). The snow-temperature relationship is also effected by the snowpack, due to melting snow and consequent increases in latent heat, and vegetation cover, which acts to limit the role of snow cover and snow melt (Chapin III et al., 2005; Mote, 2008).

https://doi.org/10.5194/esd-2019-36
Preprint. Discussion started: 23 July 2019

Climate model simulations have shown differences in the regions with the strongest snow-temperature relationship, with some studies looking at North America finding the strongest links between temperature and snow cover over parts of eastern North America (e.g. Xu and Dirmeyer, 2011), and others suggesting northwestern U.S. and southern Canada (e.g. Dutra et al., 2011). Many of the uncertainties related to biases within climate model simulations are related to the land cover parameterizations within the models, such as how the models capture the masking effect of vegetation on snow cover (Loranty et al., 2014; Qu and Hall, 2014). Evaluating the differences between climate model simulations of snow cover, surface albedo and their influences may help to improve future projections of warming.

This paper is structured by first evaluating a selection of Coupled Model Intercomparison Project phase 5 (CMIP5) climate models (Taylor et al., 2012) against an observational dataset in terms of their ability to capture recent warming rates of seasonal cold extremes relative to corresponding mean temperatures. This is followed by discussing predicted future changes in the suite of climate models used. Next, the possible physical mechanisms driving the enhanced warming of cold extremes relative to seasonal means are explored. The investigated variables are chosen based on evidence that has been suggested by prior studies, as previously discussed. We follow an approach similar to Donat et al. (2017), assessing conditions on the day on which the cold extreme occurs, or the average of days prior to day of the extreme.

2. Data and Methods

2.1 Observational and CMIP5 data

We use the Hadley Centre Global Historical Climatology Network-Daily (HadGHCND) dataset (Caesar et al., 2006) to evaluate climate model simulations for the period 1950-2014. HadGHCND is a land only, daily gridded dataset of daily maximum and minimum temperatures from ground stations, for which daily mean temperatures are calculated by taking the average of each daily maximum and minimum temperature value for each grid cell.

The HadGHCND data are used to evaluate six individual CMIP5 models (see Table 1), which were selected based on their data availability for all of the daily climate variables being investigated. While we only show a single simulation from each model (r1i1p1), multiple ensemble runs were analysed (where available) to determine model robustness and assess internal climate variability within the models. Results of multiple ensemble runs were found to be highly correlated in both spatial pattern and magnitude of simulated changes (not shown), indicating that sensitivity of the results to internal variability within the models is small. Historical model simulations (1950–2005) are merged with Representative Concentration Pathway 8.5 (RCP8.5) simulations (2006–2099) to assess changes between the mid-20th century and early 21st century (1950-2014), as well as between the mid-20th century and late 21st century (1950-2099). For analysis of recent decades, a bilinear remapping technique is used to re-grid all models to the grid cell size of HadGHCND, that is, 2.5° latitude x 3.75° longitude, and masked to only cover land regions where sufficient observational data are available. We define ‘sufficient’ as being grid cells with at least 80% of daily data available over 1950-2014, as well as at least 50% of data available for the first and last ten years of observational data. For analysis of future projected changes, all models are re-gridded to a common grid size of 2.5° latitude x 2.5° longitude to enable inter-model comparison.

2.2 Methods

https://doi.org/10.5194/esd-2019-36
Preprint. Discussion started: 23 July 2019

For each model simulation as well as HadGHCND, daily temperature anomalies are calculated relative to a mean annual cycle of daily mean temperatures based on the entire period of analysis (1950–2014 for analysis of recent changes, and 1950–2099 for analysis of future changes). The data are then split into seasons, December to February (DJF), March to May (MAM) and September to November (SON), and all analyses are only applied to Northern Hemisphere land areas north of 30°N. For this study, we do not include boreal summer in our analysis as it was previously found to have only small changes in cold extremes relative to the mean that were less robust across a suite of CMIP5 models (Gross et al., 2019).

For each grid cell in each dataset, the seasonal minima of daily temperature anomalies are calculated annually for 1950–2014 and 1950–2099 separately, accounting for the differences in base period selection. The seasonal minima are then averaged over two periods, 1950–1981 and 1982–2014 for analysis of recent changes, and 1950–1979 and 2070–2099 for analysis of future changes, to calculate changes in the anomalously coldest days. Changes in seasonal mean temperature is similarly computed from daily mean temperature data. The difference between changes in the seasonal minima and changes in the seasonal mean is then calculated, hereafter referred to as 'excess changes'. 'Recent excess changes' refer to excess changes between the mid-20th century and early 21st century, while 'future excess changes' refer to excess changes between the mid-20th century and late 21st century. Local significance of future excess changes is assessed by a Kolmogorov-Smirnov test (KS-test) at the 5% level.

To investigate the possible drivers of the enhanced warming of seasonal cold extremes relative to the mean in the mid- to high-latitude Northern Hemisphere regions, we assess several variables available at the daily time-scale in the selected CMIP5 models. This includes daily data for snow cover (CMIP5 variable name *snc*), snow amount (*snw*) and upwelling and downwelling longwave and shortwave radiation fluxes at the surface (*rlus*, *rlds*, *rsus*, *rsds*). We also assess surface albedo, calculated as the ratio of upwelling shortwave radiation and downwelling shortwave radiation, and horizontal temperature advection, which is derived for each model using the equation:

$$Tadv = u \times \left(\frac{dT}{dlon}\right) + v \times \left(\frac{dT}{dlat}\right)$$

where u and v are the zonal and meridional wind components (*uas* and *vas*, respectively), and dT is the local absolute daily mean temperature gradient in the zonal and meridional direction. For surface albedo, there are some instances in high-latitude regions where values are unrealistically large, as a result of low incoming shortwave radiation values that affect the calculation of surface albedo. In any instance where surface albedo values are outside of the physically reasonable 0 to 1 range, values are set to missing. Several other daily variables were also assessed, such as surface heat fluxes and cloud cover, but were found of low relevance as potential drivers of cold extremes in the seasons and regions being examined.

The analysis of the physical mechanisms related to the enhanced warming of cold extremes is limited to future changes, where the signal is stronger than for recent changes, and therefore shows a more robust identification of relationships. For each of the variables assessed, except temperature advection, data are evaluated on the specific day when the seasonal minima occurs. For temperature advection, a three-day average prior to the day the cold extreme occurs is used. This is because it is likely that larger changes in circulation would have more of an influence on temperature in the days leading up to the event, rather than the day of the event. Days leading up to the cold event were also examined for the other variables, but results showed no clear difference compared to using values on the exact day of the event. Excess changes are also calculated for each variable in much the same way as temperature, by taking the difference between the value of the variable on the days of the temperature extreme (or three-day average prior for temperature advection) and the seasonal mean of the

https://doi.org/10.5194/esd-2019-36
Preprint. Discussion started: 23 July 2019

variable. In essence, this removes the mean from the analysis and shows regions that experience increases or decreases in conditions related entirely to the days on which the cold extremes occur.

Results of the physical relationships are presented in two ways: one by showing maps of the variables as is shown for excess changes in temperature (to infer on the similarity of spatial patterns), and the other by showing scatter plots of correlations of future excess changes in cold extremes with either snow cover or albedo. The former is included in supplementary material due to the number of figures while the latter are included within the main body of the manuscript. For the scatter plots, annual 'excess' values for the two time periods used for the future analysis are calculated as the difference between the variable value on the day the seasonal minima occurs and the seasonal mean of the respective variable. Weighted area-averages of the annual excess values are then calculated for all grid boxes within a selected region that adhere to a specified condition that only includes grid cells that have a statistically significant future excess change exceeding 1°C. Two regions are assessed, one covering North America, and the other covering much of northern Eurasia, and are common to all models (see Fig. S1). Regressions are calculated using total least squares regression, with correlation coefficients computed using Spearman's rank correlation.

3. Results

3.1 Recent changes in cold extremes relative to the mean

Excess changes between recent decades in seasonal cold extremes relative to corresponding mean temperatures are shown for HadGHCND and individual CMIP5 models for DJF (Fig. 1), MAM (Fig. 2) and SON (Fig. 3). In all figures, and subsequent maps of excess changes, positive values indicate regions where cold extremes have warmed more than the mean, while negative values indicate regions where cold extremes have warmed less than the mean. Global pattern correlations are shown in the top right above each map, indicating the spatial similarity between each model with HadGHCND.

Pattern correlations between the observations and the individual CMIP5 models are low, indicating differences in the spatial patterns, however, this may be due to the relatively low magnitude of excess change and high spatial noise across the observations and models over the past 60 years. During winter (Fig. 1), the observations and most of the individual models agree that cold extremes have warmed more than the mean for parts of Canada and Alaska, as well as parts of western Europe, and central Asia, although the exact locations of these excess changes differ (as reflected in the low pattern correlations). Springtime (Fig. 2) show slightly higher pattern correlations between observations and the models, with all models, excluding INM-CM4, showing even higher correlations in autumn (Fig. 3). Compared with winter, MAM and SON generally show stronger and more widespread positive excess changes over Europe and Eurasia. For most of the models, the strongest excess changes overall are shown for parts of Russia/Eurasia, especially during the shoulder seasons, except for CanESM2 which shows particularly strong positive excess changes in DJF in central/eastern Europe. In the observations, the strongest excess changes are shown for much of Eurasia in SON and DJF, but mostly central Europe and North America during MAM.

Despite the generally low pattern correlations between the models and observations, the same general pattern of excess change in cold extremes is apparent, with the most prominent positive excess changes in recent decades occurring in the northern continental interiors for all seasons shown. This motivates us to assess projections of enhanced warming of cold extremes in the selected six climate models over the Northern Hemisphere extratropics.

https://doi.org/10.5194/esd-2019-36
Preprint. Discussion started: 23 July 2019

209
210 **3.2 Projected excess changes in cold extremes between future and past decades**
211
212 Projections of excess changes in cold extremes comparing the mid-20th century with the late 21st century are shown for each
213 of the six individual CMIP5 models for DJF (Fig. 4), MAM (Fig. 5) and SON (Fig. 6). Stippling over grid cells specifies
214 where changes are statistically significant, as assessed by a KS-test. Much of the Northern Hemisphere extratropics indicate
215 that cold extremes are projected to warm significantly more than mean temperatures. For winter (Fig. 4), CanESM2 shows
216 the most prominent excess changes, covering much of North America, eastern and central Europe, and northern Eurasia.
217 While not quite as strong, all other models show mostly significant positive excess changes in cold extremes for many of the
218 same regions, particularly Alaska, eastern Canada, and eastern and central Europe. There is some variation over northern
219 Russia/Siberia, with CNRM-CM5 showing significant negative excess changes around -1.5°C, opposed to relatively strong
220 positive excess changes around 3°C shown in CanESM2, MPI-ESM-LR and MPI-ESM-MR. As in the recent excess
221 changes, spring and autumn generally show a more widespread and systematic pattern of positive excess changes over
222 Eurasia, Canada and Alaska. In MAM (Fig. 5), the models show some differences in the southern parts of the U.S. and
223 Eurasia, which mostly show non-statistically significant negative excess changes. There is relatively good agreement
224 between models for the strong excess changes over much of the Eurasian and Russian region during MAM, except for INM-
225 CM4 which shows smaller and mostly non-significant positive excess changes for the northern half of Russia. In terms of
226 model agreement, SON (Fig. 6) is similar to MAM, with the greatest model agreement over Alaska, Canada and
227 central/eastern Europe and northern Eurasia, excluding non-significant small excess changes in northern Russia for CSIRO-
228 Mk3-6-0. For Alaska, northern Canada and northern Eurasia, positive excess changes are generally largest for SON
229 compared with the other seasons, except CanESM2 which shows particularly large excess changes in DJF.
230
231 Overall, future excess changes are robust and systematic across the models in winter, spring and autumn, with many mid- to
232 high-latitude regions projecting enhanced warming in cold extremes relative to the mean. To explore the possible physical
233 mechanisms driving the enhanced warming of cold extremes, we focus on the regions that show the most robust signals. The
234 strongest excess changes across all the shown seasons are over northern Eurasia and northern North America. This is
235 relatively consistent with the largest recent excess changes occurring in the northern continental interiors in observations and
236 CMIP5 models, though is much more widespread and systematic in the predicted patterns.
237
238 **3.3 Projected changes in cold air temperature advection prior to cold extremes**
239
240 Due to the evidence suggesting Arctic amplification, and consequent changes in thermal advection, as a main driver of
241 decreasing temperature variability in Northern Hemisphere regions (e.g. Screen and Simmonds, 2010; Screen, 2014;
242 Schneider et al., 2015; Holmes et al., 2016; Rhines et al., 2017), we first consider projections of changes in cold air
243 temperature advection for the three days prior to the cold event. Figure 7 shows future changes in actual and excess cold air
244 temperature advection in the CanESM2 model. Results for the remaining models are included as Supplementary
245 Material (Figs. S2 – S3), with any key differences between the models highlighted below.
246
247 The most notable features occur for DJF, which shows reductions in cold air temperature advection for much of North
248 America as well as Eurasia. This is evident for changes in both actual and excess cold air temperature advection, which
249 suggests the changes are related to a change in the overall mean state of cold air temperature advection, rather than changes
250 associated with the days directly prior to the day the cold extreme occurs. This is similarly true for the other models (see
251 Figs. S2 – S3), however, the magnitude of reduction in cold air temperature advection is generally larger in CanESM2

https://doi.org/10.5194/esd-2019-36
Preprint. Discussion started: 23 July 2019

compared with the other models. This is reflected in future excess changes in cold extremes, where CanESM2 is generally warmer than the other models for DJF. For much of the central and eastern U.S., reductions in cold air temperature advection of at least -2°C are projected for the late 21st century, with the same areas showing the largest positive excess changes in cold extremes. This is indicative of reductions in cold air temperature advection, both related to the day of the extreme as well as changes in the mean-state, being a dominant driver of the enhanced warming of cold extremes relative to the mean during boreal winter (see Fig. 4). Similarly, the greatest decreases in cold air temperature advection over the European continent occur in Scandinavia and Eurasia, which also show high magnitude excess warming in cold extremes during DJF. This same pattern is evident across all of the selected climate models. Though some reductions in cold air temperature advection are shown scattered over North America and Eurasia for MAM and SON, the spatial pattern does not match with the seasonal future excess changes in cold extremes like DJF does.

Based on these results, it is evident that a reduction in cold air temperature advection is driving the projected excess changes in cold extremes over much of North America and Eurasia during winter. Both shoulder seasons, however, while also showing substantial negative correlations between cold air advection and excess cold extremes, have a less clear signal with generally smaller values in cold air temperature advection, pointing to other mechanisms as a more dominant driver of the enhanced warming of cold extremes in spring and autumn months.

3.4 Projected changes in snow cover and surface albedo associated with cold extremes

Many of the grid cells showing significantly strong excess changes are located in regions that experience high snow fall. Snow cover and associated surface albedo feedbacks therefore play a major role in temperature variability in these regions, but it is not clear if this relationship extends to the accelerated warming of cold extremes relative to local mean temperatures, and the seasonal influence remains uncertain. The subsequent results show scatter plots of excess changes in cold extremes and snow cover (Fig. 8) and surface albedo (Fig. 9). As outlined in Sect. 2.2, these changes are calculated for the exact day when the cold extreme occurs. Projections of changes in actual and excess snow cover and surface albedo for the days of the cold extreme are included as Supplementary Material (Figs. S4-S5 and S8-S9, respectively). For additional information on the snow-temperature relationship, future changes in snow amount are also included as Supplementary Material (see Figs. S6-S7).

For both regions, mostly significant negative correlations between snow cover and excess cold extremes are shown for all seasons, aside from excess snow cover in DJF. For the North America region (Fig. 8a-f), while all models show significant negative correlations of at least -0.74 for actual snow cover in DJF (Fig. 8a), all models except CSIRO-Mk3-6-0 show significantly positive correlations for excess snow cover in DJF (Fig. 8b). From Figs. S4 – S5, parts of North America, particularly southern Alaska, southern Canada and along the north-western coast of the U.S., show projected decreases in actual snow cover, but slight increases in excess snow cover. This suggests that the feedback between snow cover and the projected enhanced warming of cold extremes is related to overall reductions in the mean snow cover over winter, rather than decreases in snow cover specifically on the day of the extreme only. For MAM and SON, negative correlations are stronger for both actual snow cover (Fig. 8c,e) and excess snow cover (Fig. 8d,f), compared to DJF, and are the strongest for SON. Again, this is reflected in the maps, where actual snow cover is projected to decrease around 40% for much of Alaska and northern Canada during autumn months, while decreasing somewhat less and slightly further south during spring (Fig. S4). Smaller decreases are projected for excess snow cover for many of the same regions, excluding Alaska which shows mostly small positive increases during spring (Fig. S5).

https://doi.org/10.5194/esd-2019-36
Preprint. Discussion started: 23 July 2019

Northern Eurasia (Fig. 8g-l) shows similar correlations to that of North America. The overall largest correlations between snow cover and excess cold extremes occur in SON (Fig. 8k,l), with some models, for example CanESM2 and CNRM-CM5, showing correlations as high as -0.91 between actual snow cover and excess cold extremes, and decreases over 45% for parts of western Russia and Scandinavia (Fig. S4). Correlations are slightly lower for actual snow cover in MAM (Fig. 8i), with the largest decreases in snow cover occurring in Scandinavia and central/eastern Europe, and no substantial changes in northern Russia (Fig. S4). This is reflected in projected changes in snow amount (Fig. S6), with increases shown for regions showing no changes in snow cover. Correlations with excess snow cover in MAM are substantially smaller for most models, with parts of northern Russia showing small increases in snow cover (Fig. S5) and snow amount (Fig. S7).

Decreases in snow cover imply that reductions in surface albedo are a likely factor contributing to the enhanced warming of cold extremes relative to the mean. Correlations between surface albedo and excess temperature (Fig. 9) indeed show strong similarities with those of snow cover, with the largest negative correlations shown for SON for both North America (Fig. 9a-f) and northern Eurasia (Fig. 9g-l). As for snow cover, the strongest overall decreases are shown for actual changes in surface albedo over Alaska, northern Canada and Eurasia during autumn months (Fig. S8). Differences in the magnitude and sign between actual surface albedo and excess surface albedo are also clear. For example, mostly positive correlations with excess surface albedo are shown for DJF for both regions (Fig. 9b,h). During boreal winter in high-latitude regions, solar insolation is low, and so it is expected that surface albedo, which is calculated using shortwave radiation fluxes, is less of a factor in driving excess changes in temperature during these months.

There is a clear relationship between decreases in snow cover, associated lower albedo and the enhanced warming of cold extremes for many regions in the Northern Hemisphere mid- to high-latitudes. While negative correlations are shown for actual snow cover and excess cold extremes during winter for both North America and Eurasia, projected decreases in actual snow cover, as shown in the maps in Fig. S4, are generally much smaller than they are for both shoulder seasons, especially autumn months which show the overall largest decreases and highest correlations with excess temperatures in cold extremes. Much of this relationship between snow cover, surface albedo and excess temperatures in cold extremes is a consequence of overall decreases in the mean-state of both snow cover and surface albedo, rather than decreases in snow cover specifically on the day in which the cold extreme occurs. This is consistent across the selection of CMIP5 models used in this study.

3.5 Projected changes in the timing of anomalously cold days

The enhanced warming of cold extremes projected for much of the Northern Hemisphere mid- to high-latitudes is clearly related to excess heat near the land surface that acts to decrease the severity of the anomalously coldest days of the season. During spring and autumn, much of this is likely a consequence of less snow and lower albedo, leading to increases in absorbed shortwave radiation at the surface and consequently amplifying the warming of cold extremes, creating a positive feedback. In addition to these relationships presented above, we also analysed an increase in net radiation on the days of the cold extremes in both shoulder seasons, with increases in incoming shortwave radiation being the largest contributor (not shown). These increases are, however, largely attributable to temporal shifts in the occurrence of the largest negative temperature anomalies in the shoulder seasons.

Figure 10 shows the projected change in the timing of the seasonal minimum of daily anomalies during MAM and SON, as simulated in CanESM2 (see Fig. S10 for all models and seasons). For much of the Northern Hemisphere mid- to high latitudes, excluding the most southerly parts, the Mediterranean region and parts of Greenland, the anomalously coldest days are projected to occur later in the season during MAM (Fig. 10a). In some regions, such as central-western Europe and

https://doi.org/10.5194/esd-2019-36
Preprint. Discussion started: 23 July 2019

eastern Canada, the anomalously coldest spring days are projected to occur more than 30 days later in the late 21st century, compared to those simulated in the mid-20th century. For SON (Fig. 10b), the anomalously coldest days are projected to shift to earlier in the season for most high latitude regions in the Northern Hemisphere. For example, the anomalously coldest days are projected to occur over 30 days earlier than they did in the mid-20th century much some regions in northern Canada and northern Eurasia. This change in the timing of cold extremes suggests an overall flattening of the seasonal cycle in these extratropical Northern Hemisphere regions. Coupled with the cold extremes warming at a faster rate than average temperatures, this suggests these regions will experience generally longer duration warmer months and a shorter duration of colder months.

4. Discussion and conclusions

Cold extremes are projected to warm more than seasonal average temperatures for much of the Northern Hemisphere mid- to high-latitude regions, for all seasons except boreal summer. Though these projected changes differ slightly in magnitude and spatial pattern depending on the CMIP5 model used, the most prominent excess changes are robust across the selection of models. These changes are likely related to projected changes in horizontal temperature advection, snow cover and surface albedo feedbacks. The season in which the excess changes in cold extremes occur largely dictates which physical mechanisms are at play.

Decreases in snow cover and lower surface albedo are more associated with excess changes in cold extremes during spring and autumn months. Due to low solar insolation in winter months, and subsequently only small effects from changes in shortwave radiation and surface albedo, reductions in cold air temperature advection in the days leading up to the extreme event is the dominant driver during boreal winter. This latter finding is likely a consequence of Arctic amplification and is in agreement with previous studies linking the warming of cold days in winter months with warmer than usual air being brought from the Arctic to lower latitudes (e.g. Screen, 2014; Schneider et al., 2015; Holmes et al., 2016; Rhines et al., 2017).

In contrast, Arctic warming and associated sea ice loss has been argued to result in more persistent severe cold air outbreaks over continental regions in the mid-latitudes during boreal winter (e.g. Kodra et al., 2011; Cohen et al., 2014, 2018; Francis and Vavrus, 2015; Zhang et al., 2016). Recent cold snaps in the United States and Eurasia, such as those observed in the boreal winter of 2012/2013, can largely be explained by a southward shift in the jet stream and a weakening of the stratospheric polar vortex (Francis and Vavrus, 2015; Zhang et al., 2016; Cohen et al., 2018; Kretschmer et al., 2018). Though some argue these events are likely transient and related to atmospheric decadal variability (e.g. Barnes and Screen, 2015; Ayarzagüena and Screen, 2016; Sun et al., 2016), others suggest that severe cold snaps in the Northern Hemisphere mid-latitudes might persist in response to continued Arctic warming (e.g. Kodra et al., 2011; Francis and Vavrus, 2012, 2015; Cohen et al., 2014). While there is some disagreement between models and observations in how they simulate the observed cold outbreaks (e.g. Cohen et al., 2013; Sun et al., 2016), there is robust model agreement that mid-latitude cold extremes are projected to decrease in severity (Screen, 2014; Barnes and Screen, 2015; Screen et al., 2015a, b; Ayarzagüena and Screen, 2016). Some have also suggested that cold air outbreaks will decrease in duration and frequency (e.g. Screen et al., 2015a, b), however, this remains unclear and requires further work (e.g. Ayarzagüena and Screen, 2016). Though the results in this study cannot infer anything regarding the frequency and duration of cold spells, it is evident that cold extremes are projected to warm in excess of increasing mean temperatures over North America and Eurasia during boreal winter by the end of the 21st century.

https://doi.org/10.5194/esd-2019-36
Preprint. Discussion started: 23 July 2019


Earth System Dynamics Discussions
Open Access
EGU

Arctic amplification and associated thermal advection is also suggested to be a particularly strong driver of decreased cold extremes in autumn months (e.g. Screen, 2014; Holmes et al., 2016). While significant negative correlations between cold air temperature advection and excess cold extremes are shown for all models for both North America and Eurasia during autumn (see Fig. 7), reductions in cold air temperature advection are substantially less coherent than they are for winter (see Figs. S2-S3). This highlights that area-averaged correlations are sometimes misleading in terms of exploring the processes driving temperature extremes over a large region. While Arctic amplification and associated reductions in cold air temperature advection may be having somewhat of an impact on the warming of cold extremes during the shoulder seasons, other physical mechanisms likely have a greater influence on changes in spring and autumn cold extremes.

For both shoulder seasons, 'hot spots' of enhanced warming of cold extremes relative to the mean are shown for much of Alaska, Canada and northern Eurasia (Figs. 5-6). During autumn, snow cover shows an exceptionally similar spatial pattern to excess changes in cold extremes for all models (see Fig. S4 and Fig. 6, respectively), with the largest excess changes in cold extremes matching regions showing the largest decreases in snow cover. Spatial similarities between snow cover and excess changes in cold extremes during spring are less obvious than they are for autumn, with slightly lower correlations, though the largest decreases in snow cover are still associated with significant excess changes in cold extremes (see Fig. S4 and Fig. 5). Previous work has suggested that spring has the strongest snow-temperature relationship, largely due to increases in latent heat from snowmelt (e.g. Dutra et al., 2011; Xu and Dirmeyer, 2011; Diro et al., 2018). Many of the regions showing the strongest relationship between projected snow cover and the projected amplification of warming cold extremes, such as northwestern U.S., southern and northeast Canada and the Rocky Mountains, are in agreement with historical simulations of the snow-temperature association during winter and spring months (Dutra et al., 2011; Diro et al., 2018). While some high-latitude regions in northern Canada and northern Russia show projected increases in snow amount during spring (see Figs. S6-S7), with the same regions and seasons showing no substantial changes in snow cover (see Figs. S4-S5), correlations between snow and excess temperature in autumn are generally larger. This infers that even if springtime is associated with a stronger snow-temperature relationship, due to increases in snowmelt, decreases in snow cover have more of an influence on warming anomalously cold days in autumn months.

A change in surface albedo feedback, as a result of a change in snow cover, is more likely to influence cold days in winter and early spring due to peak snow accumulation during this time. While results presented here show projections of decreasing albedo for many regions in North America and Europe, autumn shows the largest decreases in surface albedo (see Fig. S8), which is closely related to the projected decreases in snow cover. We note that our calculation of surface albedo, as simply the ratio between absorbed and reflected shortwave radiation, may not be capturing certain aspects that are important to snow affected areas. For example, the boreal forest is a region with extensive snow fall and dense vegetation cover, and the varying land parameterizations within the climate models may not necessarily be capturing the snow that is intercepted by trees in the canopy (Loranty et al., 2014; Thackeray et al., 2015). This then has important implications on surface albedo and therefore surface temperature.

Biases in climate model simulations of snow-albedo feedbacks have been found over the boreal forest region, with significant underestimations compared with observations, especially during periods where snowmelt is high, such as in early March (Fletcher et al., 2012; Loranty et al., 2014; Qu and Hall, 2014; Thackeray et al., 2014, 2015). However, biases in the models are reduced over larger study regions (Thackeray et al., 2015), with area-averaging over large regions also likely to suppress any biases. Biases may also simply be a consequence of temperature, with cold biases having more snow, and warm biases leading to more snowmelt. The ability of climate models to capture snow-albedo feedbacks is also complicated

https://doi.org/10.5194/esd-2019-36
Preprint. Discussion started: 23 July 2019

by factors relating to snow type and the ageing of snow, which can also influence surface temperatures (Thackeray et al., 2015; Diro et al., 2018). Improving the ability of climate models to capture realistic changes in snow cover and surface albedo would enable more accurate projections of future cold extremes. Biases in the representation of physical relationships may control the simulation of long-term changes in cold extremes. Given the availability of suitable observations of relevant land variables, an evaluation of the land-atmosphere relationships as outlined here may serve to develop process-based constraints to reduce the uncertainty in future projections, similar to previous approaches focussing on the processes driving hot extremes in summer (Donat et al., 2018).

While our findings are consistent with the theory that less snow cover and associated reductions in surface albedo lead to anomalously warmer temperatures on cold days, it is unclear whether these variables are driving the enhanced warming of cold extremes, or vice versa. It is true, however, that the positive feedback between snow cover, surface albedo and surface temperature exacerbate the warming of cold extremes. It would be useful for future studies to run climate model simulations with and without snow cover prescribed to quantify the specific impact on simulated cold extremes, enabling more confident conclusions regarding snow cover and albedo as a driver of enhanced cold extremes.

Similar to albedo, radiative fluxes are strongly influenced by changes in the surface which affects the overall surface energy budget. Decreases in snow cover which lead to lower albedo will result in increased absorption of incoming shortwave radiation for regions and seasons with enough solar insolation. While we did find some increases in incoming shortwave radiation on the days when the coldest anomalies occur, this is more an artefact of the timing in which the cold extreme occurs. For high-latitude regions, the seasonal minimum in spring time is projected to occur later in the season, with the autumn minima projected to occur earlier in the season, suggesting an overall flattening of the seasonal cycle. Changes in the annual cycle of surface temperature have been detected before, with a shift to earlier seasons by 1.7 days shown for extratropical land regions in recent decades (Stine et al., 2009). Further, changes in the seasonal cycle have been projected by CMIP3 models too, with colder tempreatures occuring later and warmer temperatures occuring earlier, reducing the amplitude of the seasonal cycle (Dwyer et al., 2012). These shifts are argued to be a consequence of anthropogenic climate change driving sea ice loss (Dwyer et al., 2012), but have also been linked with changes in the Northern Annular Mode (Stine et al., 2009).

The day the cold extreme occurs is also associated with less snow, albeit largely due to decreases in mean snow cover, so it can be inferred that the snow will likely melt more as well, as it is occurring closer to summer months than normal. This describes another positive feedback within the system, with snowmelt leading to increases in latent heat which in turn heat the surface. This highlights the fact that multiple factors within the surface energy budget are contributing to an overall greater heating at the surface, thus influencing the decrease in the severity of cold days relative to mean warming during spring and autumn months.

The enhanced warming of seasonal cold extremes relative to seasonal mean temperature is projected for much of the Northern Hemisphere mid- to high-latitudes. The main findings of this paper show that the possible drivers of this enhanced warming depend on the season. Reductions in cold air temperature advection, likely as a consequence of Arctic amplification, are the most probable driver of enhanced cold extremes during winter months. For boreal autumn and spring, snow cover and surface albedo feedbacks are the most likely contributors affecting the accelerated warming rates of cold extremes. These findings are robust across the selection of CMIP5 models used in this study. While observational data were used to evaluate simulations of excess temperature in recent decades, the climate variables are only explored as future changes, with model agreement suggesting how robust changes are. Future work in understanding the physical mechanisms

driving cold extremes would benefit in evaluating observational data of snow cover against model simulations. Further, regional climate models would provide finer-scale information that would be more useful for future planning.

Author contributions

MHG was responsible for almost all the writing and analysis during the preparation and submission process of this manuscript, with contributions from all co-authors.

Data availability

HadGHCND data can be downloaded for free at http://www.metoffice.gov.uk/hadobs/hadghcnd/download.html. All CMIP5 data are available from the public CMIP5 archive and can be downloaded at https://esgf-node.llnl.gov/search/cmip5.

Competing interests

The authors declare that there are no conflicts of interest.

Acknowledgments

This study was supported by the Australian Research Council (ARC) Centre of Excellence for Climate Extremes (Grant CE170100023). MGD received funding from the ARC (Grant DE150100456). We acknowledge the World Climate Research Programme's Working Group on Coupled Modelling, which is responsible for CMIP, and we thank the climate modelling groups (listed in Table 1 of this paper) for producing and making their model output available.

References

Ayarzagüena, B., and Screen, J. A.: Future Arctic sea ice loss reduces severity of cold air outbreaks in midlatitudes, Geophys. Res. Lett., 43, 2801–2809, doi: 10.1002/2016GL068092, 2016.

Barnes, E. A., and Screen, J. A.: The impact of Arctic warming on the midlatitude jet-stream: Can it? Has it? Will it?, Wiley Interdiscip. Rev. Clim. Chang., 6, 277–286, doi: 10.1002/wcc.337, 2015.

Brown, S. J., Caesar, J., and Ferro, C. A. T.: Global changes in extreme daily temperature since 1950, J. Geophys. Res, 113, D05115, doi: 10.1029/2006JD008091, 2008.

Caesar, J., Alexander, L., and Vose, R.: Large-scale changes in observed daily maximum and minimum temperatures: Creation and analysis of a new gridded data set, J Geophys Res, 111, D05101, doi: 10.1029/2005JD006280, 2006.

Chapin III, F., Sturm, M., Serreze, M., McFadden, J. P., Key, J. R., Lloyd, A. H., McGuire, A. D., Rupp, T. S., Lynch, A. H., Schimel, J. P., Beringer, J., Chapman, W. L., Epstein, H. E., Euskirchen, E. S., Hinzman, L. D., Jia, G., Ping, C.-L., Tape, K. D., Thompson, C. D. C., Walker, D. A., and Welker, J. M.: Role of land-surface changes in Arctic summer warming, Science, 310, 657–660, doi: 10.1126/science.1117368, 2005.

Cohen, J., and Rind, D.: The effect of snow cover on the climate, J Clim, 4, 689–706, 1991.

Cohen, J., Jones, J., Furtado, J.C., and Tziperman, E.: Warm Arctic, cold continents: A common pattern related to Arctic sea ice melt, snow advance, and extreme winter weather, Oceanography, 26, 150–160, doi: 10.5670/oceanog.2013.70, 2013.

Cohen, J., Screen, J. A., Furtado, J. C., Barlow, M., Whittleston, D., Coumou, D., Francis, J., Dethloff, K., Entekhabi, D., Overland, J., and Jones, J.: Recent Arctic amplification and extreme mid-latitude weather, Nat Geosci, 7, 627–637, doi: 10.1038/ngeo2234, 2014.

Cohen, J., Pfeiffer, K., and Francis, J. A.: Warm Arctic episodes linked with increased frequency of extreme winter weather in the United States, Nat Commun, 9, 1–12, doi: 10.1038/s41467-018-02992-9, 2018.

https://doi.org/10.5194/esd-2019-36
Preprint. Discussion started: 23 July 2019

510 Diro, G. T., Sushama, L., and Huziy, O.: Snow-atmosphere coupling and its impact on temperature variability and extremes
511 over North America, Clim Dyn, 50, 2993–3007, doi: 10.1007/s00382-017-3788-5, 2018.
512 Donat, M. G., and Alexander, L. V.: The shifting probability distribution of global daytime and night-time temperatures,
513 Geophys Res Lett, 39, L14707, doi: 10.1029/2012GL052459, 2012.
514 Donat, M. G., Alexander, L. V., Yang, H., Durre, I., Vose, R., Dunn, R. J. H., Willett, K. M., Aguilar, E., Brunet, M.,
515 Caesar, J., Hewitson, B., Jack, C., Klein Tank, A. M. G., Kruger, A. C., Marengo, J., Peterson, T. C., Renom, M., Oria
516 Rojas, C., Rusticucci, M., Salinger, J., Elrayah, A. s., Sekele, S. S., Srivastava, A. K., Trewin, B., Villarroel, C.,
517 Vincent, L. A., Zhai, P., Zhang, X., and Kitching, S.: Updated analyses of temperature and precipitation extreme
518 indices since the beginning of the twentieth century: The HadEX2 dataset, J Geophys Res Atmos, 118, 2098–2118,
519 doi: 10.1002/jgrd.50150, 2013.
520 Donat, M. G., Pitman, A. J., and Seneviratne, S. I.: Regional warming of hot extremes accelerated by surface energy fluxes,
521 Geophys Res Lett, 44, 7011–7019, doi: 10.1002/2017GL073733, 2017.
522 Donat, M. G., Pitman, A. J., and Angélil, O.: Understanding and reducing future uncertainty in midlatitude daily heat
523 extremes via land surface feedback constraints, Geophys Res Lett, 45, 10,627-10,636, doi: 10.1029/2018GL079128,
524 2018.
525 Dutra, E., Schär, C., Viterbo, P., and Miranda, P. M. A.: Land-atmosphere coupling associated with snow cover, Geophys
526 Res Lett, 38, L15707, doi: 10.1029/2011GL048435, 2011.
527 Dwyer, J. G., Biasutti, M., and Sobel, A. H.: Projected changes in the seasonal cycle of surface temperature, J Clim, 25,
528 6359–6374, doi: 10.1175/JCLI-D-11-00741.1, 2012.
529 Fletcher, C. G., Zhao, H., Kushner, P. J., and Fernandes, R.: Using models and satellite observations to evaluate the strength
530 of snow albedo feedback, J Geophys Res Atmos, 117, D11117, doi: 10.1029/2012JD017724, 2012.
531 Francis, J. A., and Vavrus, S. J.: Evidence linking Arctic amplification to extreme weather in mid-latitudes, Geophys Res
532 Lett, 39, L06801, doi: 10.1029/2012GL051000, 2012.
533 Francis, J. A., and Vavrus, S. J.: Evidence for a wavier jet stream in response to rapid Arctic warming, Environ Res Lett, 10,
534 014005, doi: 10.1088/1748-9326/10/1/014005, 2015.
535 Gross, M. H., Donat, M. G., Alexander, L. V., and Sisson, S. A.: The sensitivity of daily temperature variability and
536 extremes to dataset choice, J Clim, 31, 1337–1359, doi: 10.1175/JCLI-D-17-0243.1, 2018.
537 Gross, M. H., Donat, M. G., and Alexander, L. V.: Changes in daily temperature extremes relative to the mean in Coupled
538 Model Intercomparison Project Phase 5 models and observations, Int J Climatol, 1-19, doi: 10.1002/joc.6138, 2019.
539 He, T., Liang, S., and Song, D.-X.: Analysis of global land surface albedo climatology and spatial-temporal variation during
540 1981-2010 from multiple satellite products, J Geophys Res Atmos, 119, 10,281-10,298, doi: 10.1002/2014JD021667,
541 2014.
542 Holmes, C. R., Woollings, T., Hawkins, E., and de Vries, H.: Robust future changes in temperature variability under
543 greenhouse gas forcing and the relationship with thermal advection, J Clim, 29, 2221–2236, doi: 10.1175/JCLI-D-14-
544 00735.1, 2016.
545 IPCC: Summary for policymakers, in: Managing the risks of extreme events and disasters to advance climate change
546 adaptation. Special Report of the Intergovernmental Panel on Climate Change, edited by: Field, C. B., Barros, V.,
547 Stocker, T. F., Qin, D., Dokken, D. J., Ebi, K. L., Mastrandrea, M. D., Mach, K. J., Plattner, G.-K., Allen, S. K.,
548 Tignor, M., and Midgley, P. M., 3-21, Cambridge University Press, Cambridge, UK and New York, NY, USA, 2012.
549 Kharin, V. V., and Zwiers, F. W.: Estimating extremes in transient climate change simulations, J Clim, 18, 1156–1173, doi:
550 10.1175/JCLI3320.1, 2005.
551 Kodra, E., Steinhaeuser, K., and Ganguly, A. R.: Persisting cold extremes under 21st-century warming scenarios, Geophys
552 Res Lett, 38, L08705, doi: 10.1029/2011GL047103, 2011.

https://doi.org/10.5194/esd-2019-36
Preprint. Discussion started: 23 July 2019

Kretschmer, M., Coumou, D., Agel, L., Barlow, M., Tziperman, E., and Cohen, J.: More-persistent weak stratospheric polar vortex states linked to cold extremes, Bull Am Meteorol Soc, 99, 49–60, doi: 10.1175/BAMS-D-16-0259.1, 2018.

Loranty, M. M., Berner, L. T., Goetz, S. J., Jin, Y., and Randerson, J. T.: Vegetation controls on northern high latitude snow-albedo feedback: Observations and CMIP5 model simulations, Glob Chang Biol, 20, 594–606, doi: 10.1111/gcb.12391, 2014.

Mearns, L. O., Katz, R. W., and Schneider, S. H.: Extreme high-temperature events: Changes in their probabilities with changes in mean temperature, J Clim Appl Meteorol, 23, 1601–1613, doi: 10.1175/1520-0450(1984)023<1601:EHTECI>2.0.CO;2, 1984.

Mote, T. L.: On the role of snow cover in depressing air temperature, J Appl Meteorol Climatol, 47, 2008–2022, doi: 10.1175/2007JAMC1823.1, 2008.

Qu, X., and Hall, A.: On the persistent spread in snow-albedo feedback, Clim Dyn, 42, 69–81, doi: 10.1007/s00382-013-1774-0, 2014.

Rhines, A., McKinnon, K. A., Tingley, M. P., and Huybers, P.: Seasonally resolved distributional trends of north american temperatures show contraction of winter variability, J Clim, 30, 1139–1157, doi: 10.1175/JCLI-D-16-0363.1, 2017.

Schneider, T., Bischoff, T., and Plotka, H.: Physics of changes in synoptic midlatitude temperature variability, J Clim, 28, 2312–2331, doi: 10.1175/JCLI-D-14-00632.1, 2015.

Screen JA, and Simmonds I (2010) The central role of diminishing sea ice in recent Arctic temperature amplification. Nature 464:1334–1337. doi: 10.1038/nature09051, 2010.

Screen, J. A., and Simmonds, I.: Exploring links between Arctic amplification and mid-latitude weather, Geophys Res Lett, 40, 959–964, doi: 10.1002/grl.50174, 2013.

Screen, J. A.: Arctic amplification decreases temperature variance in northern mid- to high-latitudes, Nat Clim Chang, 4, 577–582, doi: 10.1038/nclimate2268, 2014.

Screen, J. A., Deser, C., and Sun, L.: Reduced risk of North American cold extremes due to continued arctic sea ice loss, Bull Am Meteorol Soc, 96, 1489–1503, doi: 10.1175/BAMS-D-14-00185.1, 2015a.

Screen, J. A., Deser, C., and Sun, L.: Projected changes in regional climate extremes arising from Arctic sea ice loss, Environ Res Lett, 10, 84006, doi: 10.1088/1748-9326/10/8/084006, 2015b.

Serreze, M. C., and Francis, J. A.: The Arctic amplification debate, Clim Change, 76, 241–264, doi: 10.1007/s10584-005-9017-y, 2006.

Stine, A. R., Huybers, P., and Fung, I. Y.: Changes in the phase of the annual cycle of surface temperature, Nature, 457, 435–440, doi: 10.1038/nature07675, 2009.

Sun, L., Perlwitz, J., and Hoerling, M.: What caused the recent “Warm Arctic, Cold Continents” trend pattern in winter temperatures?, Geophys Res Lett, 43, 5345–5352, doi: 10.1002/2016GL069024, 2016.

Taylor, K. E., Stouffer, R. J., and Meehl, G. A.: An overview of CMIP5 and the experiment design, Bull Am Meteorol Soc, 93, 485–498, doi: 10.1175/BAMS-D-11-00094.1, 2012.

Thackeray, C. W., Fletcher, C. G., and Derksen, C.: The influence of canopy snow paramterizations on snow albedo feedback in boreal forest regions, J Geophys Res Atmos, 119, 9810–9821, doi: 10.1002/2014Jd021858, 2014.

Thackeray, C. W., Fletcher, C. G., and Derksen, C.: Quantifying the skill of CMIP5 models in simulating seasonal albedo and snow cover evolution, J Geophys Res Atmos, 120, 5831–5849, doi: 10.1002/2015JD023325, 2015.

Xu, L., and Dirmeyer, P.: Snow-atmosphere coupling strength in a global atmospheric model, Geophys Res Lett, 38, L13401, doi: 10.1029/2011GL048049, 2011.

Ylhäisi, J. S., Räisänen, J.: Twenty-first century changes in daily temperature variability in CMIP3 climate models, Int J Climatol, 34, 1414–1428, doi: 10.1002/joc.3773, 2014.

Zhang, J., Tian, W., Chipperfield, M. P., Xie, F., and Huang, J.: Persistent shift of the Arctic polar vortex towards the

https://doi.org/10.5194/esd-2019-36
Preprint. Discussion started: 23 July 2019

596 Eurasian continent in recent decades, Nat Clim Chang, 6, 1094–1099, doi: 10.1038/nclimate3136, 2016.
597
598

Table 1 List of CMIP5 models used in this study and their institution.

Model	Modelling group
CanESM2	Canadian Centre for Climate Modelling and Analysis (CCCMA)
CNRM-CM5	Centre National de Recherches Météorologiques / Centre Européen de Recherche et Formation Avancée en Calcul Scientifique (CNRM-CERFACS)
CSIRO-Mk3.6.0	CSIRO in collaboration with Queensland Climate Change Centre of Excellence (CSIRO-QCCCE)
INM-CM4	Institute for Numerical Mathematics (INM)
MPI-ESM-LR	Max Planck Institute for Meteorology (MPI-M)
MPI-ESM-MR	Max Planck Institute for Meteorology (MPI-M)

https://doi.org/10.5194/esd-2019-36
Preprint. Discussion started: 23 July 2019

Earth System Dynamics
Discussions
Open Access
EGU

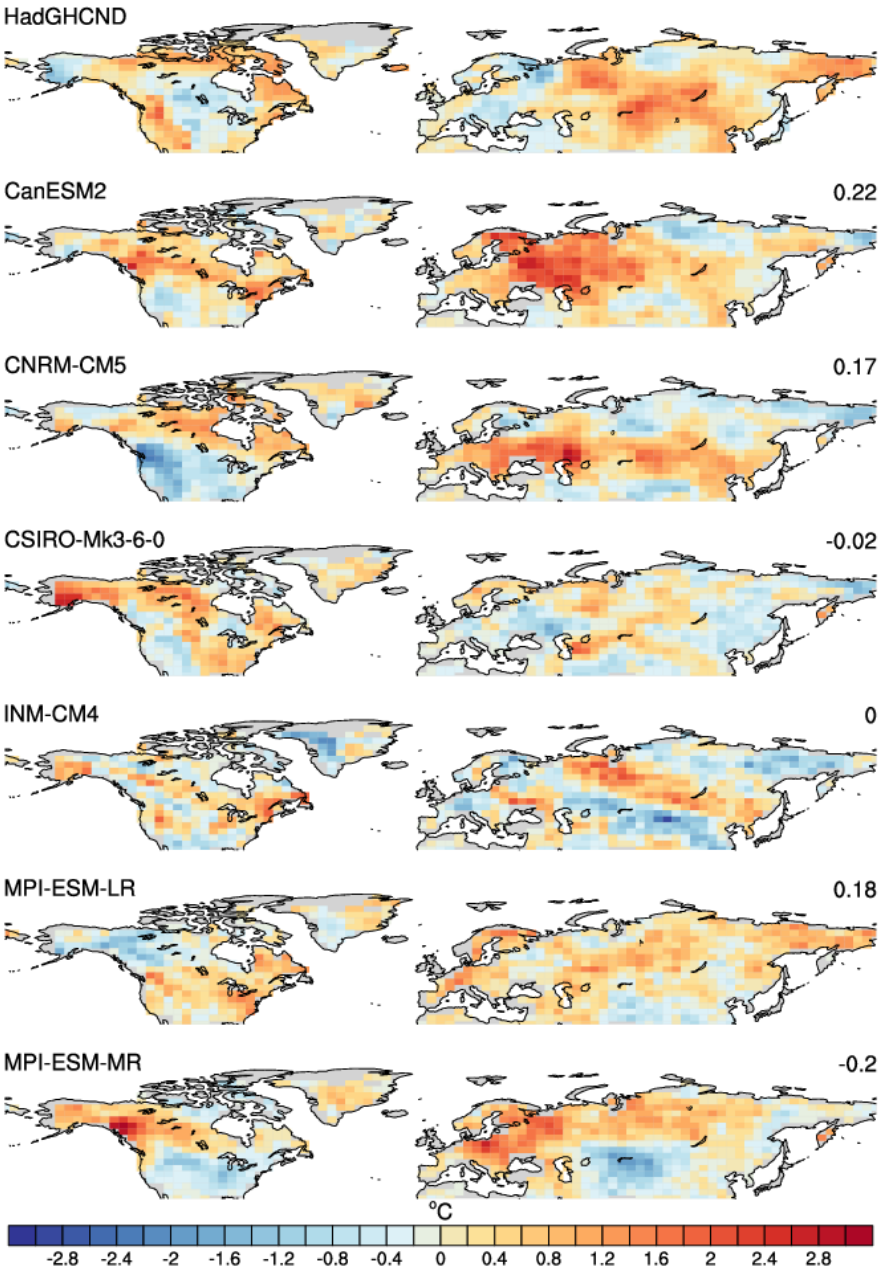

Figure 1: Recent excess changes (1982-2014 – 1950-1981) in cold extremes (seasonal minima – seasonal mean) for December – February. Grey areas represent areas where data is missing in HadGHCND. The number in the top right above the maps for each model represents the pattern correlation with that model and HadGHCND.

https://doi.org/10.5194/esd-2019-36
Preprint. Discussion started: 23 July 2019

Earth System Dynamics
Discussions
Open Access
EGU

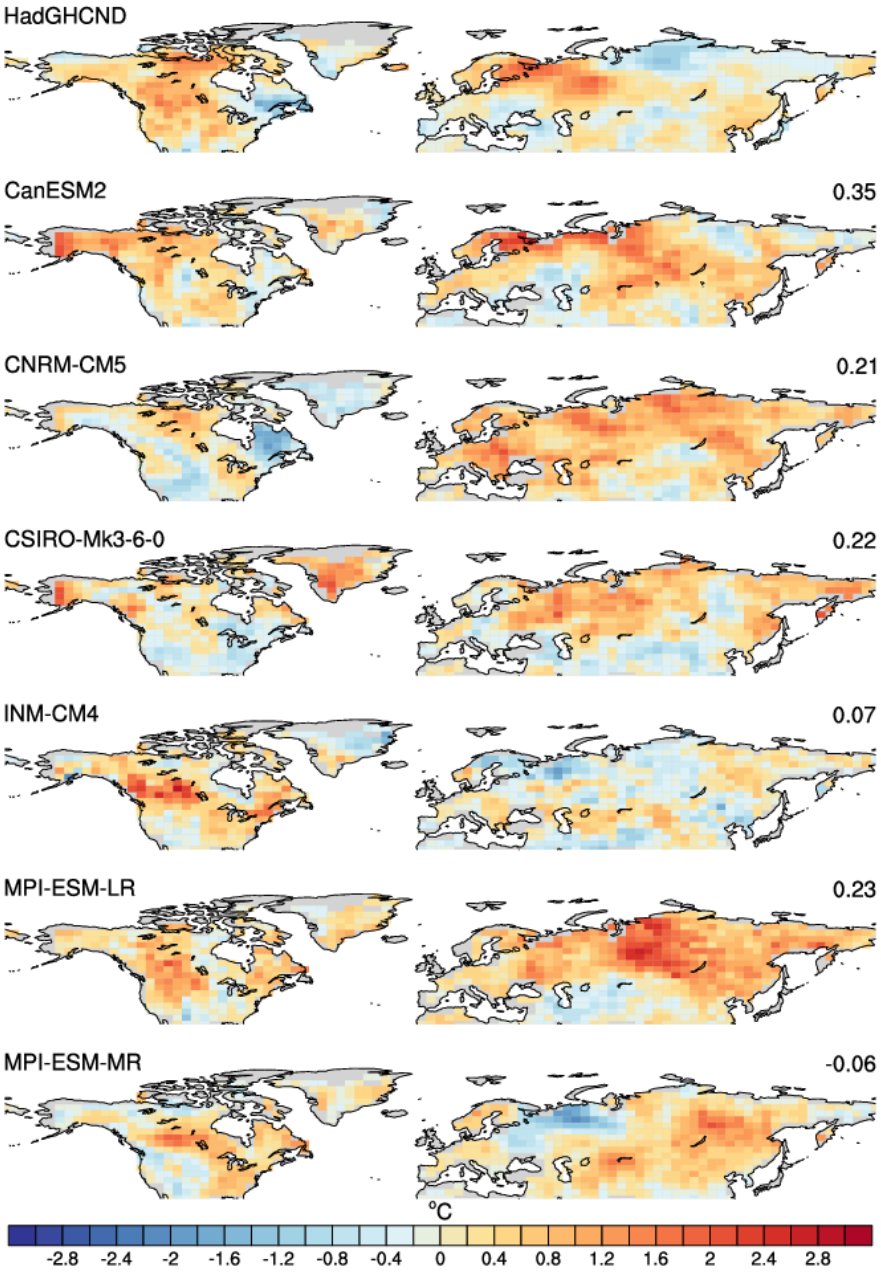

Figure 2: As Fig. 1 but for March – May.

https://doi.org/10.5194/esd-2019-36
Preprint. Discussion started: 23 July 2019

Earth System Dynamics
Discussions
Open Access
EGU

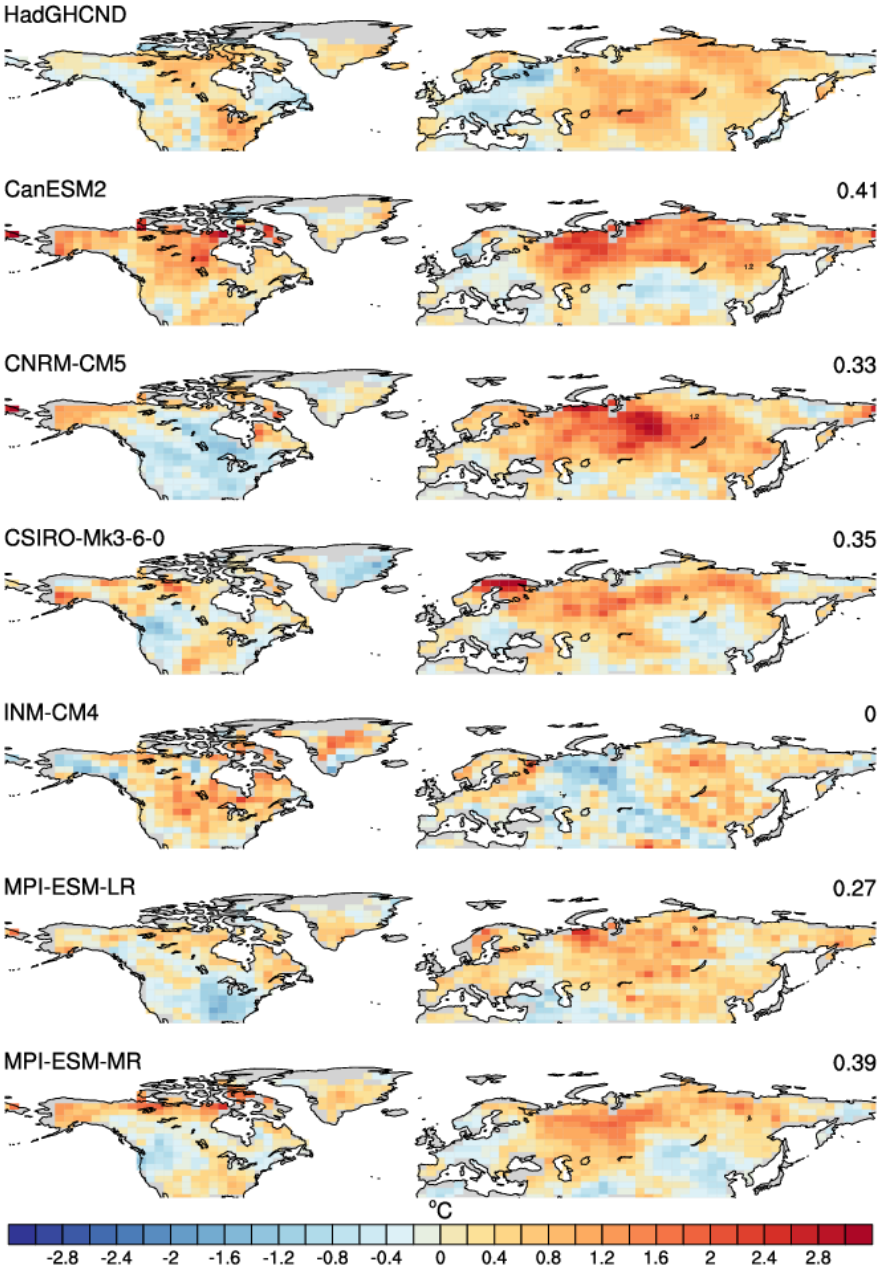

Figure 3: As Fig. 1 but for September – November.

https://doi.org/10.5194/esd-2019-36
Preprint. Discussion started: 23 July 2019

Earth System Dynamics
Discussions
Open Access
EGU

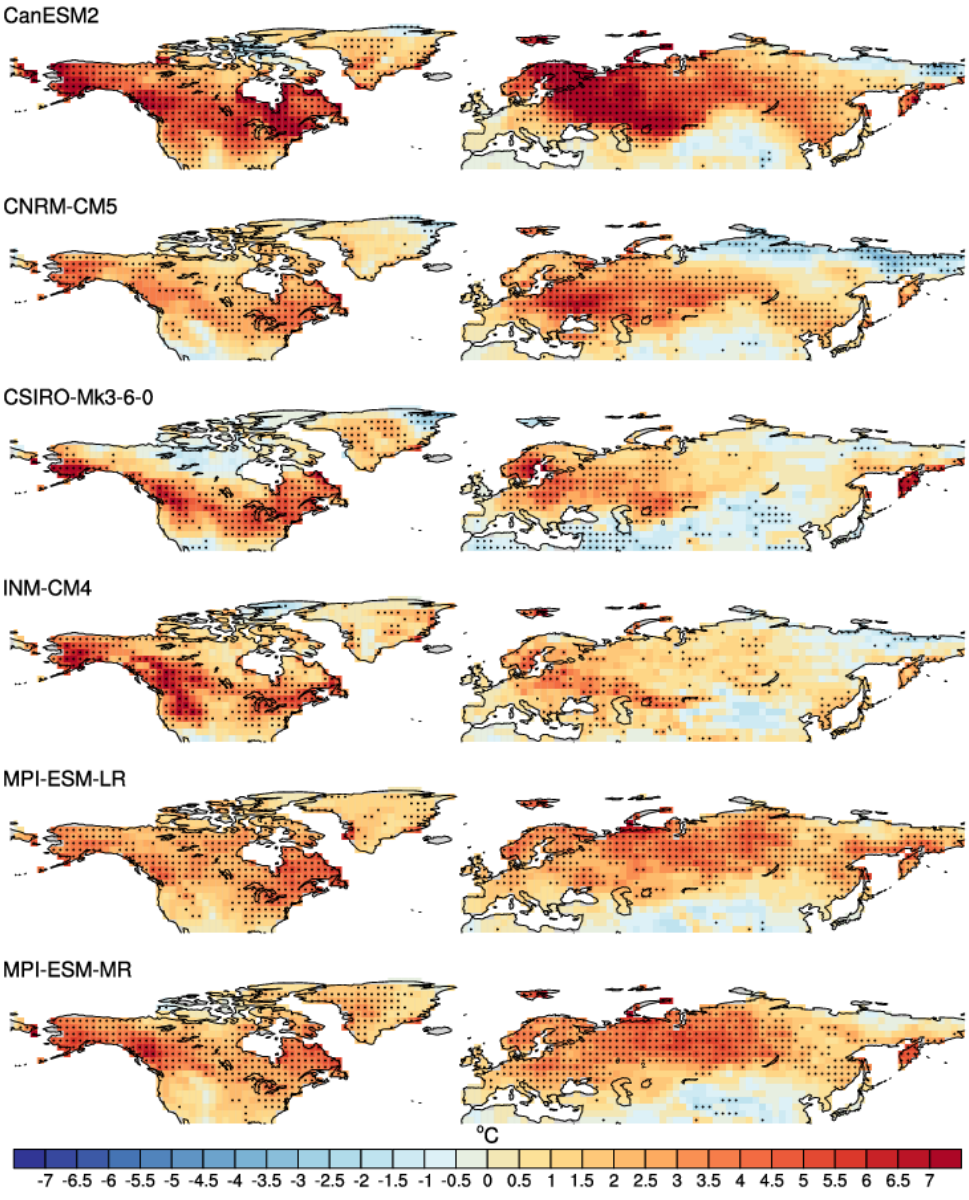

Figure 4: Future excess changes (2070-2099 – 1950-1979) in cold extremes (seasonal minima – seasonal mean) for December – February. Stippling indicates grid cells that are significant at the 5% level as assessed by a KS-test.

https://doi.org/10.5194/esd-2019-36
Preprint. Discussion started: 23 July 2019

Earth System Dynamics
Discussions
Open Access
EGU

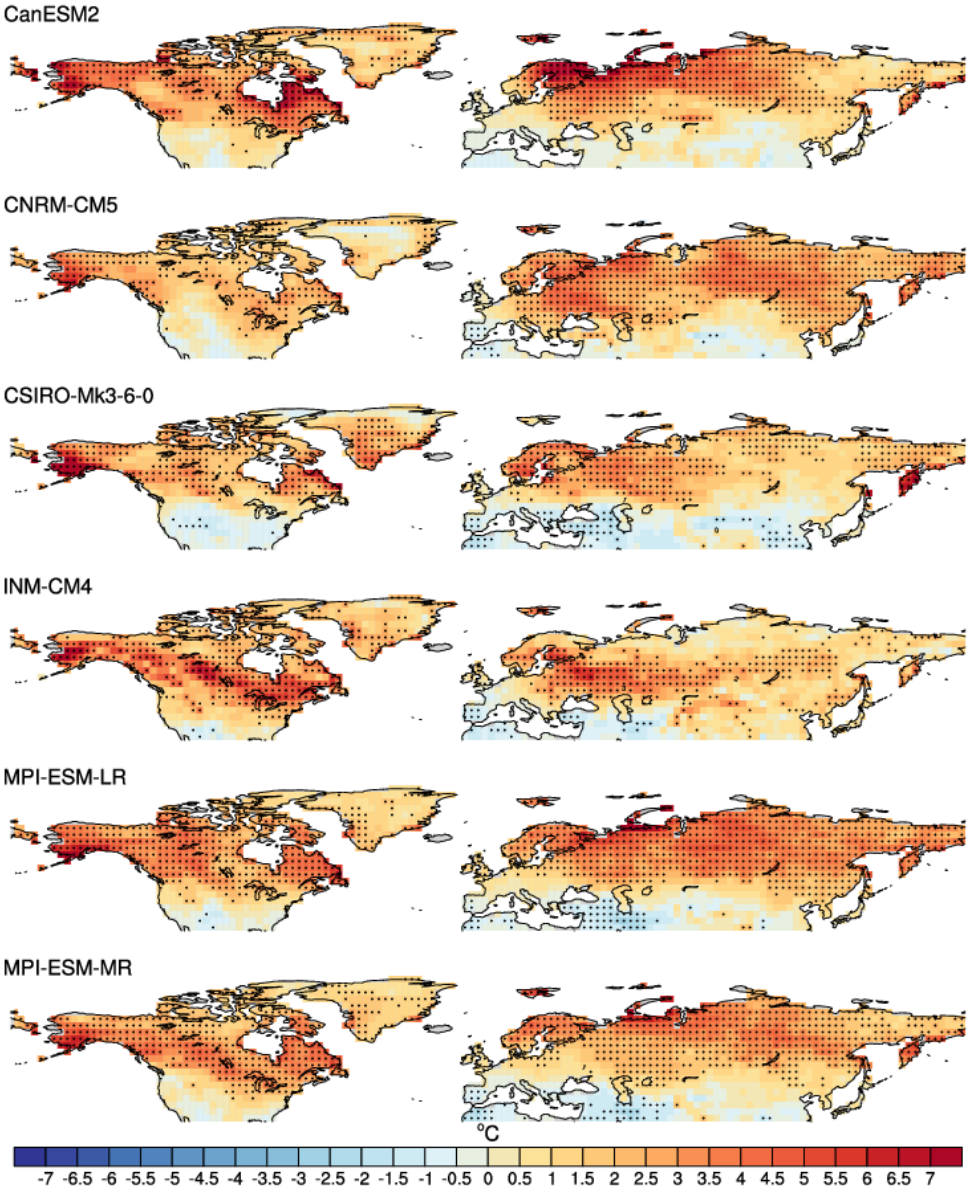

Figure 5: As Fig. 4 but for March – May.

https://doi.org/10.5194/esd-2019-36
Preprint. Discussion started: 23 July 2019

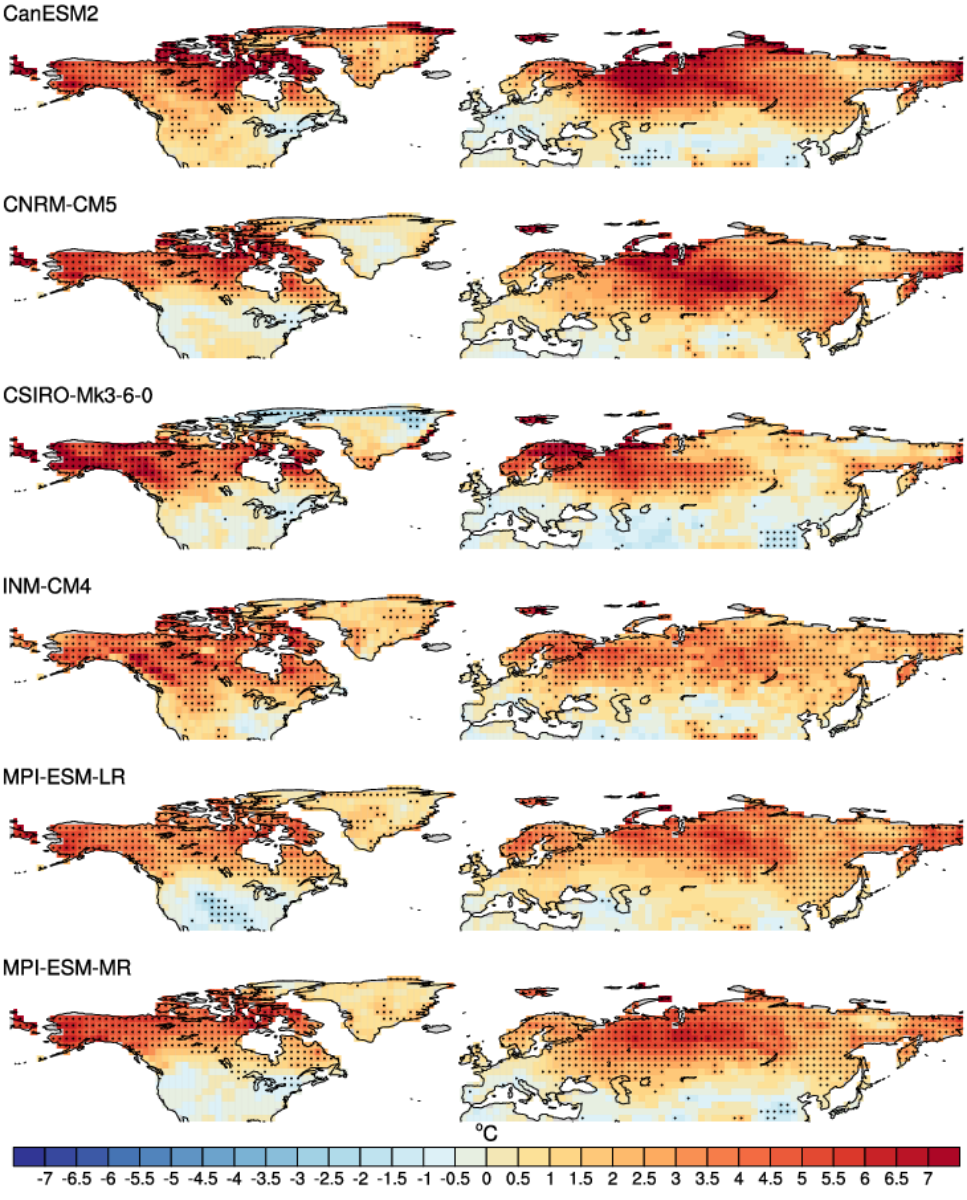

Figure 6: As Fig. 4 but for September – November.

https://doi.org/10.5194/esd-2019-36
Preprint. Discussion started: 23 July 2019

Earth System Dynamics
Discussions
Open Access
EGU

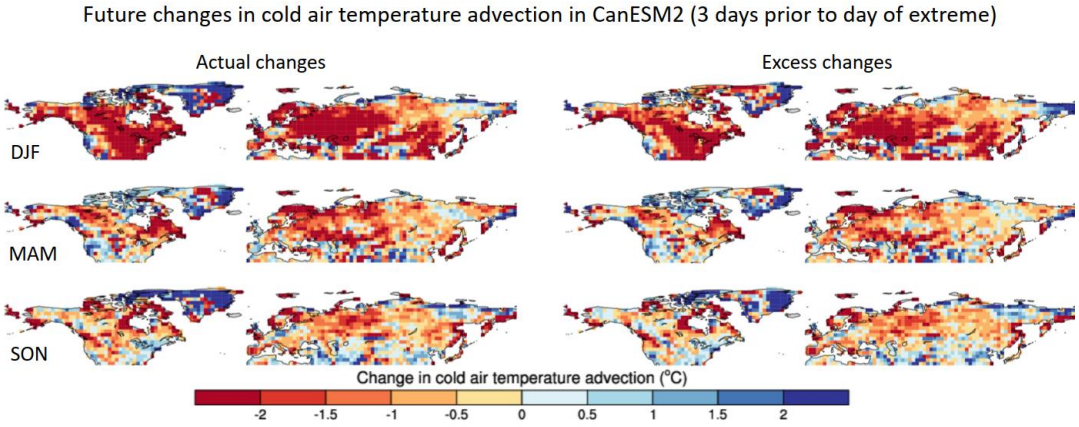

Figure 7: Future changes (2070-2099 – 1950-1979) in actual (left column) and excess (right column) cold air temperature advection for December – February (top row), March – May (middle row) and September – November (bottom row) in CanESM2. Values are calculated using the average cold air temperature advection for the three days prior to the day the annual seasonal minimum occurs, with negative values indicating reductions in cold air advection, and positive values indicating increases. All six of the selected climate models used in this study are shown in Figs. S2 – S3.

https://doi.org/10.5194/esd-2019-36
Preprint. Discussion started: 23 July 2019

Earth System Dynamics
Discussions
Open Access
EGU

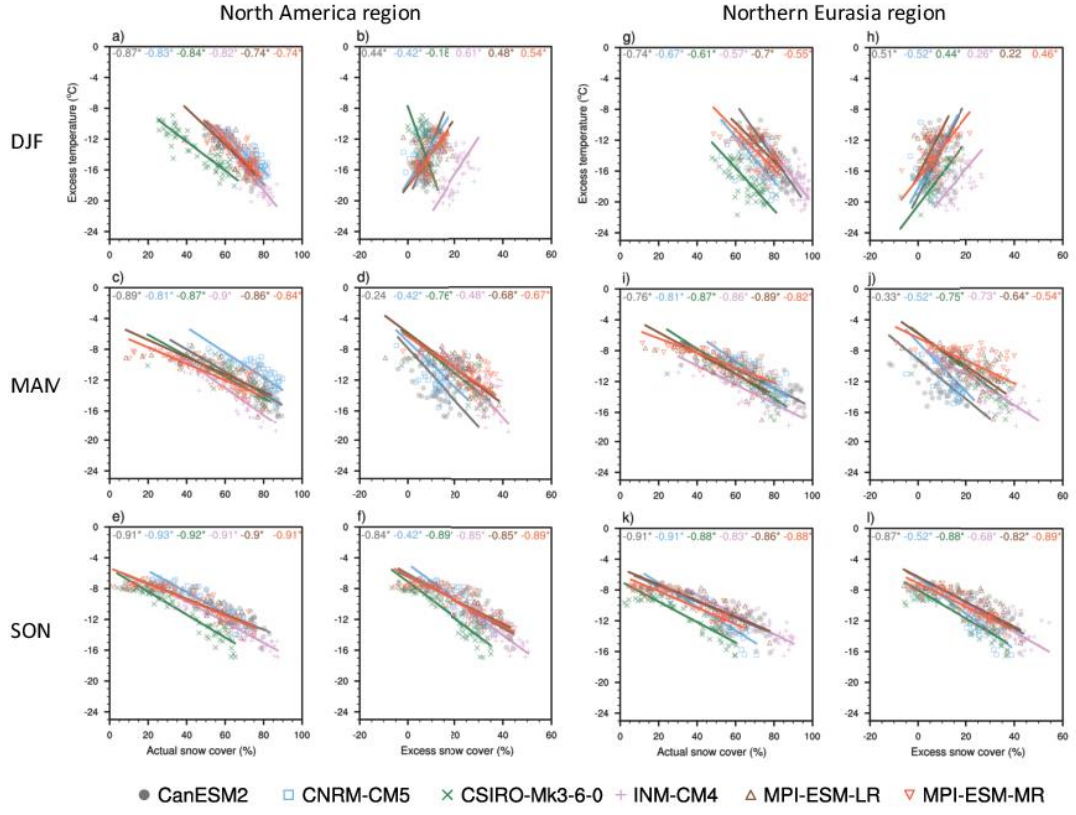

Figure 8: Scatter plots showing annual values of excess temperatures in cold extremes for each season (seasonal minima – seasonal mean) on the y-axis, and annual values in each season of actual snow cover, calculated on the day the cold extreme occurs, on the x-axis (1st and 3rd column). The 2nd and 4th column show values of excess snow cover on the x-axis (i.e. snow cover on the day of the extreme – mean annual snow cover). Each row represents a different season: December – February in the 1st row, March – May in the 2nd row, and September – November in the 3rd row. Each value is an area-average of two regions (see Fig. S1): North America (a-f) and northern Eurasia (g-l). The straight lines indicate the regression slope for each model calculated using total least squares regression. Correlation coefficients are shown at the top of each panel, with the different colours indicating the model. * indicates significance at the 5% level.

https://doi.org/10.5194/esd-2019-36
Preprint. Discussion started: 23 July 2019

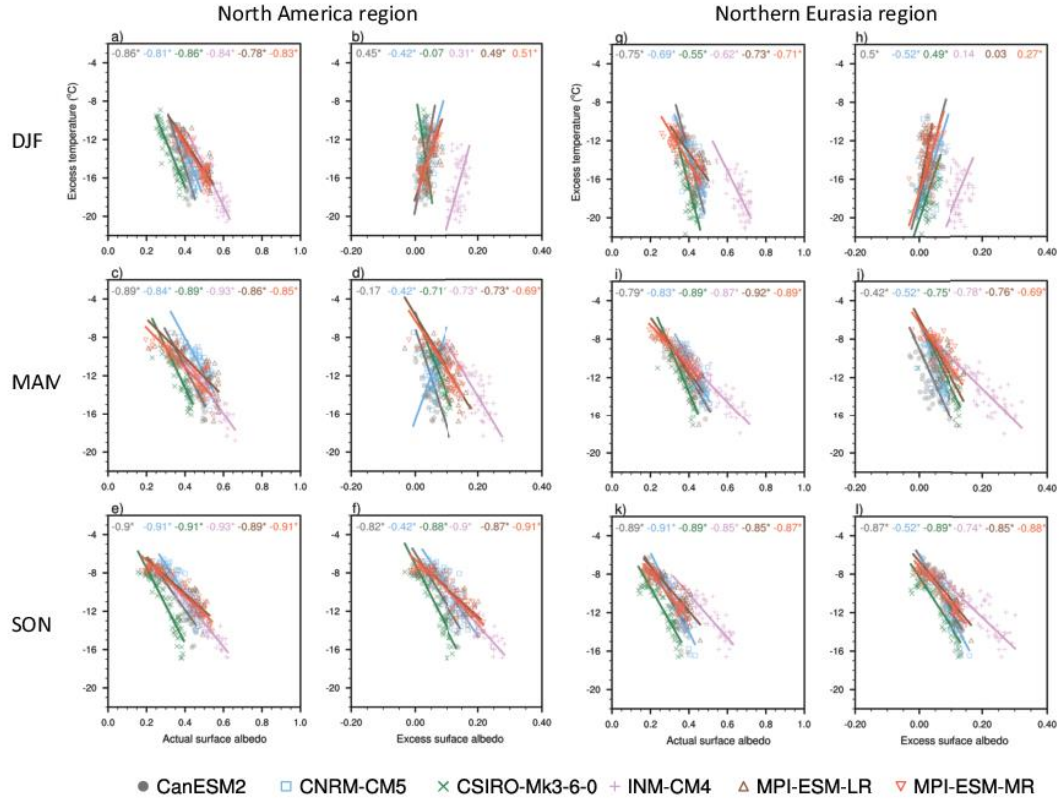

Figure 9: As Fig. 8, but for surface albedo.

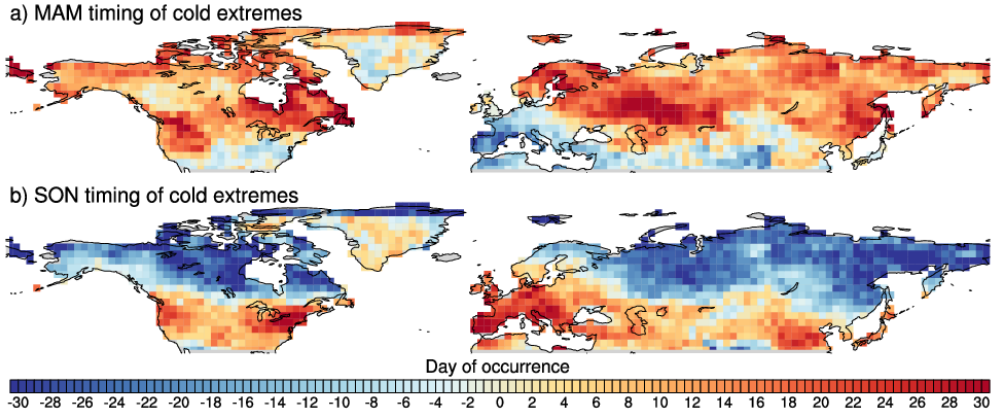

Figure 10: Changes in the timing of the anomalously coldest day in the season between 2070-2099 and 1950-1979 for March – May (a) and September – November (b), as shown for the CanESM2 model. All models and all seasons, excluding boreal summer, are shown in Fig. S10.